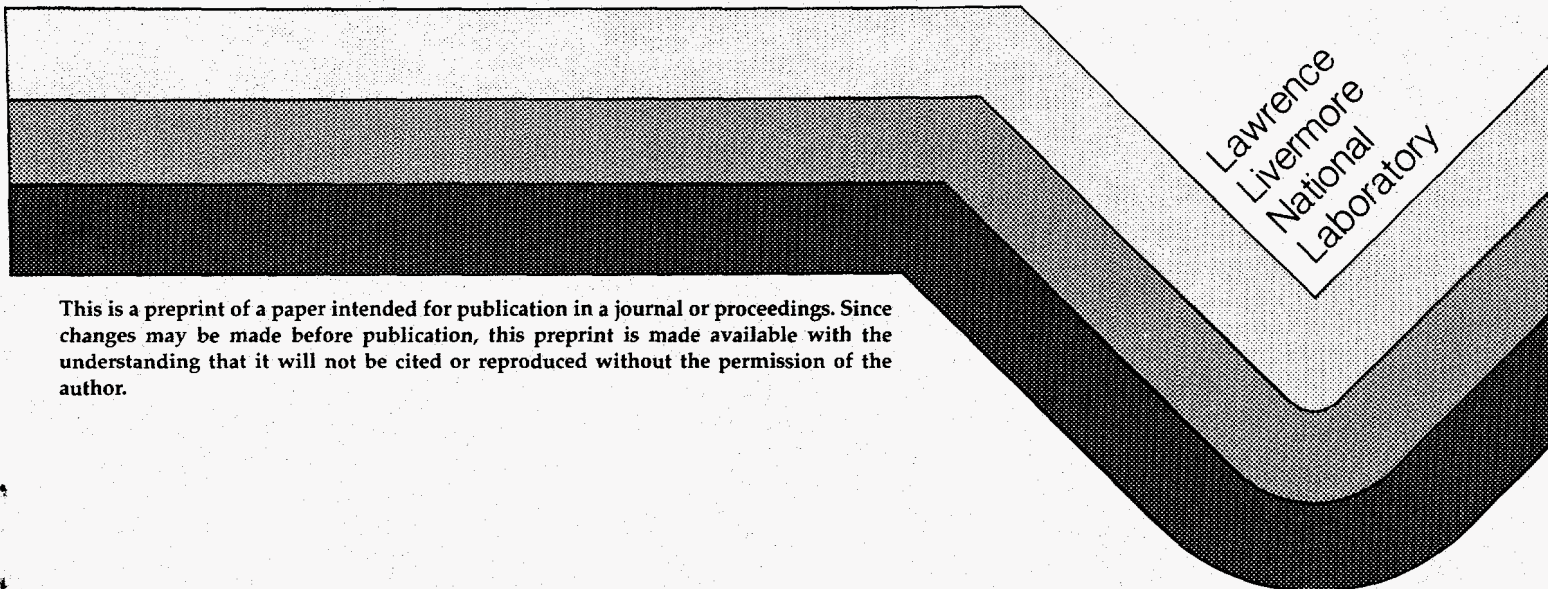# Measurements of Cross Sections and Resonance Structures Following Electron-Impact Excitation/Ionization of Na-Like Kr and Xe

D. Schneider
D. DeWitt
D. A. Knapp
K. J. Reed
M. H. Chen

Lawrence Livermore National Laboratory

DISCLAIMER

DISCLAIMER

Measurements of Cross Sections and Resonance Structures Following Electron-Impact Excitation/Ionization of Na-Like Kr and Xe

D. Schneider, D. DeWitt, D. A. Knapp, K. J. Reed, and M. H. Chen

,

High Temperature Division
Physics Department
Lawrence Livermore National Laboratory
Livermore, CA 94550 USA

ABSTRACT

We report high-resolution measurements of electron impact excitation and ionization cross sections for the Na-like ions Kr^{25+} and Xe^{43+}. Ions with ionization states centered on the Na-like configurations were produced in an electron beam ion trap (EBIT) using electrons with energies below the L shell ionization thresholds. The Na-like ions were exposed to an electron beam with an energy between 3 and 7 keV. The Na- and Ne-like ions were then extracted and their intensities measured as a function of the electron beam energy. Theoretical ionization cross sections were calculated using relativistic distorted wave methods. Complex resonance structures that appear in the computed cross sections are observed in the experimental results. These results are the first experimental observation of resonant-excitation-double-autoionization (REDA) in highly charged high-Z ions.

INTRODUCTION

In the last decade much theoretical and experimental effort has been devoted to the measurement of electron-impact ionization cross sections in highly charged ions important to studies of high temperature plasmas in astrophysics and fusion research.[1-6] Electron impact ionization affects the ionization balance, electron density, and temperature of these plasmas as well as the plasma kinetics. The electron beam ion trap (EBIT)[7,8] has proven an effective tool for studying interactions of highly charged high Z ions with electrons. X ray emission from dielectronic recombination and electron-impact excitation has been investigated for ions up to Ne-like Th^{80+}.[9-13] The installation of an ion extraction system on EBIT has allowed complementary measurements of extracted, momentum-analyzed ion yields, enabling studies of nonradiative decay channels. The evolution of ionization states in the trap as a function of electron energy[8,14] can be investigated, along with the processes of dielectronic recombination[15,16] and electron impact excitation and ionization. In this paper we report the results of a high-resolution study of electron impact ionization of Na-like Kr and Xe ions. The measured cross sections are compared to detailed theoretical calculations.

For incident electron energies below the threshold for direct L-shell ionization, a Na-like ion in the ground state can be ionized through indirect processes as well as through direct removal of the 3s electron. The most important indirect process is excitation-autoionization (EA), which occurs when an inner-shell electron is excited to an $n = 3$ or $n = 4$ orbital by inelastic electron-ion scattering, followed by Auger decay of the excited state. This results in a distinctive step-wise rise in the ionization cross section near the threshold for the excitation. Another important indirect process is resonant excitation followed by sequential double autoionization (REDA). The REDA process for Na-like ions can be represented schematically by

$$
\begin{aligned}
e^- + 1s^2\, 2l^8\, 3s \quad &\rightarrow 1s^2\, 2l^7\, 3s\, nl\, n'l' \\
&\rightarrow 1s^2\, 2l^7\, 3s\, n''l'' + e^- \\
&\rightarrow 1s^2\, 2s^2\, 2p^6 + e^- + e^-.
\end{aligned}
$$
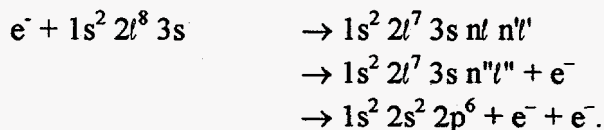
A higher order process involving a two-step resonant-excitation-auto-double-ionization (READI) can also occur.

Several theoretical studies of indirect contributions to the electron impact ionization of highly charged Na-like ions have been made in recent years.[17,18,19] They show abrupt increases in the calculated cross sections near EA thresholds. The most comprehensive calculations of REDA cross sections to date were carried out for Fe^{15+}, using a detailed multiconfiguration Dirac-Fock model.[18,19] In the calculations of the two-step double Auger branching ratios, all possible Auger channels and radiative decays leading to bound states were taken into account.[17-22] The computed ionization cross sections show complex resonance structures from the REDA process.

Electron impact ionization cross sections for Fe^{15+} have been measured using a crossed beam arrangement.[4] The observed cross sections are in general agreement with

Measurements of Cross Sections and Resonance Structures
Following Electron-Impact Excitation/Ionization of Na-Like Kr and Xe

2

the overall shape of the calculated cross sections reported in Ref. 18. However, the experiment lacked sufficient resolution to show the detailed structures predicted in the calculated cross sections. New high resolution measurements performed in a heavy ion storage ring[20] (TSR in Heidelberg, Germany) show excellent agreement with the calculated cross sections. More recently, a series of detailed high-resolution measurements employing the crossed beam technique has been performed for low-Z Li-like and Na-like ions.[6] Structures resulting from REDA and READI were reported for Li-like B^{2+} and C^{3+} and Na-like Mg^+ ions. The measurements for Li-like ions are in very good agreement with cross sections calculated using the distorted wave method and the independent process approximation[21] and also in good agreement with results of close coupling calculations.[22] Detailed measurements on low-charge heavy metal ions (e.g. La^{2+}) have shown narrow capture resonances in double, triple and quadruple ionization channels [23] and it was demonstrated that the resonance features make up about one-third of the total double ionization cross section in the case of resonant-excitation-triple autoionization (RETA).[6,23] While these experiments have shown effects for light and low-charge ions, our measurements are the first demonstration of these indirect contributions in highly charged high-Z ions.

EXPERIMENTAL

Our experimental results were obtained using the ion extraction system on the LLNL EBIT. The design and operation of EBIT and the extraction system are discussed in detail in Ref. 8. Briefly, EBIT consists of an electron beam passed through an ion trap consisting of three drift tubes. The electron beam is compressed to electron densities of about 2000 A/cm^2 by a 3 Tesla axial magnetic field in the center of the drift tubes. The voltage of the center drift tube defines the electron beam energy. Radial trapping of the ions is achieved by the space-charge of the electron beam. Axial trapping is provided by biasing the two outer drift tubes with respect to the center drift tube. Neutral gas atoms (e.g.. Kr and Xe) can be continuously injected ballistically through side ports into the trap. The gas atoms are captured and successively ionized by the beam electrons. We study electron impact excitation and ionization processes by switching the electron beam energy to an energy and intensity chosen to probe the ions. Nonradiative de-excitation processes are observed by measuring the intensity of extracted charge-state-analyzed ions as a function of electron beam energy. The fast switching between the different modes is illustrated in Fig. 1 where a schematic of timing pattern is plotted. In order to have mostly Na-like ions in the trap, the electron beam energy is switched for a short "depopulation" time interval (~100 msec) onto a dielectronic recombination resonance for Ne-like ions before the start of the actual probing cycle.

RESULTS AND DISCUSSION

Figure 2a shows the measured yields of Ne-like Xe *vs.* electron beam energy following electron impact ionization of Na-like Xe. The data clearly show an abrupt increase in the Ne-like yield at about 4.4 keV. This increase is similar to that occurring in the calculated ionization cross section from the onset of the EA process at about the same en-

Measurements of Cross Sections and Resonance Structures
Following Electron-Impact Excitation/Ionization of Na-Like Kr and Xe

3

ergy. Indeed, an increase in the ionization cross section should result in an increase in the yield of Ne-like ions. However, this measured yield represents a superposition of the dielectronic recombination process for Ne-like Xe and the ionization process for Na-like Xe ions in the trap. The rate equation for Ne-like ions, denoted N_{Ne}, is:

$$\frac{dN_{Ne}}{dt} = \underbrace{\frac{\langle j_e \rangle}{e}\sigma_{Na}^{\ I}N_{Na}}_{\text{gain}} - \underbrace{\left[\frac{\langle j_e \rangle}{e}\left(\sigma_{Ne}^{\ DR} + \sigma_{Ne}^{\ RR}\right) + \frac{1}{\tau_{Ne}}\right]N_{Ne}}_{\text{loss}}. \qquad (1)$$

At equilibrium $dN_{Ne}/dt = 0$, so that

$$\left[\frac{\langle j_e \rangle}{e}\left(\sigma_{Ne}^{\ DR} + \sigma_{Ne}^{\ RR}\right) + \frac{1}{\tau_{Ne}}\right]N_{Ne} = \frac{\langle j_e \rangle}{e}\sigma_{Na}^{\ I}N_{Na}. \qquad (2)$$

From this one obtains

$$\sigma_{Na}^{\ I} = \left[\sigma_{Ne}^{\ DR} + \sigma_{Ne}^{\ RR} + \frac{e}{\langle j_e \rangle \tau_{Ne}}\right]\frac{N_{Ne}}{N_{Na}}. \qquad (3)$$

Thus, the ionization cross section for Na-like Xe can be determined from the ratio of Ne- to Na-like Xe ions in the trap. In equation (1) $\sigma_{Ne}^{\ DR}$ is the cross section for dielectronic recombination of Ne-like ions to form Na-like ions, $\langle j_e \rangle$ is the effective electron beam current density, τ_{Ne} is the lifetime of the Ne-like state, and N_{Ne} and N_{Na} are the yields of Ne-like and Na-like ions respectively.

In Fig. 2b the ratio N_{Ne}/N_{Na} is plotted as a solid curve and shown along with the calculated ionization cross sections. The computed direct ionization cross section is shown by the dashed curve, and the dotted curve represents the EA contribution. The thick solid curve shows the calculated total ionization cross section including the REDA contribution. The solid curve, showing the ratio of Ne-like Xe to Na-like Xe, has been normalized to the direct ionization cross section in the region below threshold for the onset of EA. Thus, absolute cross sections for the total ionization of Na-like Xe can be determined from Fig. 2b.

The EA processes cause the calculated ionization cross section to increase by a factor of 5 in a series of steps between 4.4 and 5.0 keV. Since ionization transforms Xe^{43+} to Xe^{44+}, this increase in the cross section should be manifested by an increase in the ratio of Xe^{43+} to Xe^{44+} in the trap according to Eq. (3). The solid curve does indeed exhibit a series of step-like increases near the energies where increases appear in the calculated cross sections. The calculated total ionization cross section shows a complex resonance structure resulting from the superposition of the REDA contributions. Each REDA resonance was convoluted with a 20 eV FWHM Gaussian to simulate the experimental energy spread. The measured cross section also exhibits complicated structures with some peaks occurring in approximately the same positions as those in the calculated cross sections.

Measurements of Cross Sections and Resonance Structures
Following Electron-Impact Excitation/Ionization of Na-Like Kr and Xe

4

The solid curve, which represents the measured ionization cross section for Na-like Xe, also exhibits a regular series of dips resulting from dielectronic recombination resonances. Dielectronic recombination reduces the number of Ne-like ions and increases the number of Na-like ions, thereby reducing the ratio N_{Ne}/N_{Na}. When the beam energy matches the energy of a dielectronic recombination resonance a large dip appears in the solid line in Fig 2b. These are *not* dips in the ionization cross section. Fig. 3 shows the experimental dielectronic recombination spectrum for Ne-like Xe.

Although the dielectronic recombination resonances introduce complications in the measured cross sections, and although there are some differences in the detailed structures, the overall agreement between the experimental and theoretical results is good.

Fig. 4a shows the experimental yield of Ne-like Kr ions as a function of electron beam energy. In this figure, step-like increases corresponding to EA processes are apparent in the region starting about 1.75 keV. In Fig 4b the measured ionization cross sections for Na-like Kr are shown along with the calculated ionization cross sections (thick solid curve). Once again, the experimental cross sections are normalized to the cross section for direct ionization of the 3s electron. As in the case of ionization of Na-like Xe, the cross section for Na-like Kr has complicated structures, and the peaks in the measured cross section occur at the same energies for which REDA resonances occur in the calculated cross section. In this case, however, the dips caused by dielectronic recombination resonances are not as noticeable as in the case of Na-like Xe. The calculated dielectronic recombination spectrum for Ne-like Kr is shown in Fig. 5. The agreement in the positions of the peaks in the experimental and theoretical cross sections for both Kr^{25+} and Xe^{43+} suggests that these experimentally observed structures are indeed a REDA signal.

For beam energies above 2.3 keV it is possible to excite 2s electrons to $n > 3$ levels and produce autoionizing states of the ion. Near the thresholds for these excitations the ionization cross section increases abruptly and its shape is again determined by superposition of excitation-autoionization contributions to the cross section. The theoretical spectrum does not include this higher excitation/ionization threshold.

CONCLUSION

Cross sections for electron impact ionization of Na-like Kr and Xe have been determined both experimentally and theoretically. Despite complicated structure from indirect processes, the overall agreement between the measured and computed cross sections is good. Much of the structure results from dielectronic processes in Ne-like Kr and Xe. The method of measuring the energy dependence of the ionization cross sections by using the yield of extracted ions of a given charge state is well suited for studying the effects of indirect processes such as EA and REDA. These new experimental results confirm recent theoretical results that predict that these indirect contributions are of considerable importance in electron impact ionization of highly charged ions.

Measurements of Cross Sections and Resonance Structures
Following Electron-Impact Excitation/Ionization of Na-Like Kr and Xe

5

ACKNOWLEDGMENTS

Measurements of Cross Sections and Resonance Structures
Following Electron-Impact Excitation/Ionization of Na-Like Kr and Xe

6

REFERENCES

1. D. L. Moores and H. Nussbaumer, J. Phys. B **3**, 6 (1970).

2. D. H. Crandall *et al.*, Phys. Rev. A **25**, 143 (1982).

3. S. M. Younger, Phys. Rev. A **22**, 111 (1980).

4. D. C. Gregory *et al.*, Phys. Rev. A **35**, 3256 (1987).

5. D. C. Griffin, M. S. Pindzola, and C. Bottcher, Phys. Rev. A **36**, 3642 (1987).

6. A. Müller, *et al.*, Nucl. Instrum. Meth. Phys. Res. B **24/25**, 369 (1987); A. Müller, Z. Phys. D. **21**, S39 (1991).

7. R. E. Marrs *et al.*, J. Phys. (Paris) Colloq. **50**, C1-455 (1989); see also R. E. Marrs *et al.*, Phys. Rev. Lett. **60**, 1715 (1988), and D. A. Knapp *et al.*, Phys. Rev. Lett. **62**, 2104 (1989), for further description of EBIT.

8. D. Schneider *et al.*, Phys. Rev. A **42**, 3889 (1990), Phys. Rev. A (1991).

9. D. A. Knapp *et al.*, Phys. Rev. Lett. **62**, 2104 (1989).

10. P. Beiersdorfer *et al.*, Phys. Rev. Lett. **44**, 396 (1991).

11. D. A. Knapp, Z. Phys. D **21**, S143-146 (1991).

12. R. Marrs, Comm. At. Mol. Phys. **27**, 57 (1991).

13. M. Schneider *et al.*, in **Atomic Processes in Plasmas**, AIP Conf. Proc. **257**, 26 (1992).

14. B. M. Penetrante *et al.*, Phys. Rev. A **43**, 4873 (1991).

15. D. R. DeWitt *et al.*, Phys. Rev. A **44**, 7185 (1991).

16. D. R. DeWitt *et al.*, Phys. Rev. Lett. **68**, 1694 (1992).

17. K. J. Reed, Phys Rev. A **37**, 1791 (1988).

18. M. H. Chen, K. J. Reed, and D. L. Moores, Phys. Rev. Lett. **64**, 1350 (1990).

19. D. L. Moores and K. Reed, Phys. Rev. A **39**, 1747 (1989).

20. D. Habs, reported at the Nobel Symposium, Lysekil, Sweden (unpublished) (1994).

21. M. H. Chen and K. J. Reed, private communication.

22. K. J. Reed and M. H. Chen, Phys. Rev. A **45**, 4519 (1992).

23. S. S. Tayal and R. J. W. Henry, Phys. Rev. A **42**, 1831 (1990); A44, 2955 (1991).

24. A. Müller, *et al.*, Phys. Rev. Lett. **61**, 70 (1982).

Measurements of Cross Sections and Resonance Structures
Following Electron-Impact Excitation/Ionization of Na-Like Kr and Xe

7

Figure Captions.

Figure 1. Timing pattern for ionization/excitation measurements. From $t = 0$ to $t = 800$ ms the current and drift tube voltage are set to produce the ions. From $t = 800$ to $t = 1100$ ms they are switched to values appropriate to the dielectronic recombination depopulation of the Ne-like ions. At $t = 1100$ ms the drift tube voltage is adjusted to the probe energy for ionization/excitation. After $t = 1200$ ms a short extraction pulse is applied to the drift tube voltages.

Figure 2. (a) Dielectronic recombination yield of Ne-like Xe ions as a function of electron beam energy. (b) Total normalized cross sections for Na-like Xe ions as a function of electron beam energy.

Figure 3. Experimental dielectronic recombination spectrum for Ne-like Xe.

Figure 4. (a) Dielectronic recombination yield of Ne-like Kr ions as a function of electron beam energy. (b) Total normalized cross sections for Na-like Kr ions as a function of electron beam energy.

Figure 5. Theoretical dielectronic recombination spectrum for Ne-like Kr.

Measurements of Cross Sections and Resonance Structures
Following Electron-Impact Excitation/Ionization of Na-Like Kr and Xe

8

(a)

1000

Counts

100

Neonlike xenon DR

1.0

(b)   Sodiumlike xenon Ionization

Total Ionization cross section
(10⁻²⁰ cm²)

$10^{-20}\ cm^2$

0.8

0.6

0.4

0.2

0

4.0   4.2   4.4   4.6   4.8   5.0   5.2   5.4   5.6   5.8   6.0
Electron energy (keV)

JFT-U-011-26253-04

(a)

Counts

1000

200

Neonlike krypton DR

(b) Sodiumlike krypton ionization

14

12

10

8

6

4

2

0

Total Ionization cross section $(10^{-20}\ cm^2)$

1.5 1.6 1.7 1.8 1.9 2.0 2.1 2.2 2.3 2.4 2.5

Electron energy (keV)